

This discussion paper is/has been under review for the journal The Cryosphere (TC).
Please refer to the corresponding final paper in TC if available.

Seasonal cycle of solar energy fluxes through Arctic sea ice

S. Arndt and M. Nicolaus

Alfred-Wegener-Institut Helmholtz-Zentrum für Polar- und Meeresforschung, Bussestraße 24,
27570 Bremerhaven, Germany

Received: 28 April 2014 – Accepted: 19 May 2014 – Published: 5 June 2014

Correspondence to: S. Arndt (stefanie.arndt@awi.de)

Published by Copernicus Publications on behalf of the European Geosciences Union.

TCD

8, 2923–2956, 2014

**Seasonal cycle of
solar energy fluxes
through Arctic sea
ice**

S. Arndt and M. Nicolaus

Title Page

Abstract

Introduction

Conclusions

References

Tables

Figures

⏪

⏩

◀

▶

Back

Close

Full Screen / Esc

Printer-friendly Version

Interactive Discussion



Abstract

Arctic sea ice has not only decreased considerably during the last decades, but also changed its physical properties towards a thinner and more seasonal cover. These changes strongly impact the energy budget and might affect the ice-associated ecosystem of the Arctic. But until now, it is not possible to quantify shortwave energy fluxes through sea ice sufficiently well over large regions and during different seasons. Here, we present a new parameterization of light transmittance through sea ice for all seasons as a function of variable sea ice properties. The annual maximum solar heat flux of $30 \times 10^5 \text{ J m}^{-2}$ occurs in June, then also matching the under ice ocean heat flux. Furthermore, our results suggest that 96 % of the total annual solar heat input occurs from May to August, during four months only. Applying the new parameterization on remote sensing and reanalysis data from 1979 to 2011, we find an increase in light transmission of $1.5 \% \text{ a}^{-1}$ for all regions. Sensitivity studies reveal that the results strongly depend on the timing of melt onset and the correct classification of ice types. Hence, these parameters are of great importance for quantifying under-ice radiation fluxes and the uncertainty of this parameterization. Assuming a two weeks earlier melt onset, the annual budget increases by 20 %. Continuing the observed transition from Arctic multi- to first year sea ice could increase light transmittance by another 18 %. Furthermore, the increase in light transmission directly contributes to an increase in internal and bottom melt of sea ice, resulting in a positive transmittance-melt feedback process.

1 Introduction

The evolution of Arctic sea ice towards a thinner, younger and more seasonal sea ice cover during the last few decades (e.g. Comiso, 2012; Haas et al., 2008; Maslanik et al., 2011, 2007) has a strong impact on the partitioning of solar energy between the atmosphere, the sea ice, and the ocean (e.g. Perovich et al., 2007, 2011; Wang et al., 2014). A general decrease of surface albedo (Perovich et al., 2011), an earlier melt

TCD

8, 2923–2956, 2014

Seasonal cycle of solar energy fluxes through Arctic sea ice

S. Arndt and M. Nicolaus

Title Page

Abstract

Introduction

Conclusions

References

Tables

Figures

◀

▶

◀

▶

Back

Close

Full Screen / Esc

Printer-friendly Version

Interactive Discussion



Seasonal cycle of solar energy fluxes through Arctic sea ice

S. Arndt and M. Nicolaus

Title Page

Abstract

Introduction

Conclusions

References

Tables

Figures



Back

Close

Full Screen / Esc

Printer-friendly Version

Interactive Discussion



Here we present all seasons and multi-year radiation transfer through Arctic sea ice based on the work by Nicolaus et al. (2012) and (2013). We extend and generalize their up-scaling method by a new parameterization of light transmittance through various types of sea ice over the annual cycle. We also include the temporal and spatial variability of melt ponds by the application of melt-pond concentrations by Rösler et al. (2012). The timing of different seasons is derived from melt and freeze onsets from Markus et al. (2009, updated). In order to judge the reliability of the method and to obtain a measure of uncertainty, the calculated fluxes are compared to in-situ observations during the Tara drift (Nicolaus et al., 2010a) and sensitivity studies are performed. Finally, it was possible to derive trends for the years from 1979 to 2011 for radiation transfer through Arctic sea ice.

2 Methods

Solar short-wave radiation fluxes (250 to 2500 nm, here also referred to as “light”) through sea ice are calculated for the entire Arctic (north of 65° N) daily from 1 January 1979 to 31 December 2011. Starting from the method and parameterization by Nicolaus et al. (2012) and (2013) the parameterization of light transmittance through sea ice has been extended for all seasons. Transmittance is calculated as a function of sea ice type, surface (snow) melt/freeze state, and melt pond concentration. The new parameterization was merged with satellite observations of daily sea ice concentration and surface solar irradiance to calculate fluxes. All data sets are interpolated to a 10 km polar stereographic grid. Although daily fluxes are calculated and available, monthly means are shown and used to discuss the findings of this study, because we aim for seasonal changes and long-term trends.

2.1 Input data sets

The following satellite and re-analyses data sets were used (Table 1):

Seasonal cycle of solar energy fluxes through Arctic sea ice

S. Arndt and M. Nicolaus

Title Page

Abstract

Introduction

Conclusions

References

Tables

Figures

◀

▶

◀

▶

Back

Close

Full Screen / Esc

Printer-friendly Version

Interactive Discussion

1. Sea ice concentration was obtained from the Special Sensor Microwave Imager (SSM/I/S) provided through the Ocean and Sea Ice Satellite Application Facilities (OSI SAF, product ID: OSI-401, Andersen et al., 2007). For this study, the combination of reprocessed data (1979 to 2007) and operational data (2008 to 2011) was used. Both data sets have systematical differences due to the processing with a different set of tie point statistics for the ice concentration algorithm (Lavergne et al., 2010). However, within the documented uncertainties both data sets build the best available and consistent time series of sea ice concentration.
2. For sea ice age, we used the updated data product by Maslanik et al. (2007) and (2011). It is based on satellite data and a Lagrangian tracking since 1979. Although this data product distinguishes the age of the ice from 1 to 10 years, here we only distinguish FYI and MYI (2 years and older), because all MYI is assumed to have similar optical properties. All data points with a sea ice concentration > 0 but without sea ice age were treated as FYI. Vice versa, all data points with sea ice concentration < 15 % but with an age tag were treated as open water. Such modifications were necessary to obtain consistent data products from the different sources, indicating partially varying sea ice extents.
3. The downward surface solar radiation was obtained four times per day from the European Centre for Medium-Range Weather Forecast (ECMWF) Era Interim re-analyses (Dee et al., 2011). The data (four values per day) were averaged to daily means and are available since 1979.
4. Sea ice surface characteristics were categorized by melt and freeze onset dates from passive microwave data (1979 to 2012) (Markus et al., 2009, updated). The data set distinguishes between the first occurrence of a melt event (early melt onset, EMO), the following continuous melt (melt onset, MO), the first occurring of freeze-up conditions (early freeze onset, EFO), and the day of persistent freezing conditions (freeze onset, FO).

Seasonal cycle of solar energy fluxes through Arctic sea ice

S. Arndt and M. Nicolaus

Title Page

Abstract

Introduction

Conclusions

References

Tables

Figures

◀

▶

◀

▶

Back

Close

Full Screen / Esc

Printer-friendly Version

Interactive Discussion



5. Melt pond fraction was used from Rösel et al. (2012). But since this data set is only available since 2000, melt pond fractions from 1979 to 1999 were set to constant summer values of 26 % on FYI and 29 % on MYI as observed in August 2011 (Nicolaus et al., 2012). For consistencies with the surface characteristics, all melt pond fractions before EMO are set to zero.

2.2 The up-scaling model

Solar heat input through sea ice into the ocean ($E_T(t, x, y)$) is calculated as the product of the downward solar radiation (E_d), the sea ice concentration (C_i), and the total transmittance of pond covered sea ice (τ_i) for each grid cell for each day from 1 January 1979 to 31 December 1999:

$$E_T(t, x, y) = E_d(t, x, y) \times C_i(t, x, y) \times \tau_i \quad (1)$$

with time t and position (x, y) .

Since 1 January 2000, when satellite derived melt-pond concentrations are available, the solar heat input through sea ice into the ocean (E_T) is calculated as the sum of fluxes through bare ice (E_B) and melt ponds (E_P):

$$\begin{aligned} E_T(t, x, y) &= E_B(t, x, y) + E_P(t, x, y) \\ E_T(t, x, y) &= E_d(t, x, y) \times C_i(t, x, y) \times [1 - C_p(t, x, y)] \times \tau_b + E_d(t, x, y) \\ &\quad \times C_i(t, x, y) \times C_p(t, x, y) \times \tau_p \end{aligned} \quad (2)$$

with the transmitted solar radiation at the bottom of the ice E_T , downward solar radiation E_d , sea ice concentration C_i , melt pond fraction C_p , transmittance of bare sea ice τ_b , transmittance of melt ponds τ_p , time t and grid cell (x, y) .

To obtain the total solar heat input per unit area for a certain time period ($Q_T(x, y)$), the heat flux is calculated for each grid cell and then integrated over the given time (Δt)

$$Q_T(x, y) = \sum E_T(t, x, y) \Delta t. \quad (3)$$

increase was linked with the beginning of the melt phase (mean MO on 30 May 2011) and the associated strong snow melt. During this time, the difference between thin melting sea ice on the sea ice edge and the persistent sea ice cover became most obvious, e.g. in the Chuckchi and Beaufort Seas. In July, $Q_T(x, y)$ reached its maximum of $9.8 \times 10^5 \text{ J m}^{-2}$ resulting from a maximum mean transmittance of 0.089. The maximum $Q_T(x, y)$ reached still about $28 \times 10^5 \text{ J m}^{-2}$ with a Q_T of $18.4 \times 10^{19} \text{ J}$. The different impact of MYI and FYI, becomes most obvious in July. Also continuation of sea ice melt along the ice edge becomes more important for the under-ice heat fluxes. The August decrease of $Q_T(x, y)$ by more than 50% to $4.4 \times 10^5 \text{ J m}^{-2}$ along with only a slight reduction of transmittance to 0.084 is mainly caused by the strong decrease in solar surface irradiance ($679 \times 10^{19} \text{ J}$). These surface fluxes are only half of those during the previous months. Maximum $Q_T(x, y)$ reached up to $19 \times 10^5 \text{ J m}^{-2}$. In September the $Q_T(x, y)$ decreased further to $0.6 \times 10^5 \text{ J m}^{-2}$ related to a low transmittance of 0.039 and Q_T was $0.7 \times 10^{19} \text{ J}$.

3.2 Light transmission from 1979 to 2011

The new data set of $Q_T(x, y)$ allows quantification of annual budgets, regional differences, and decadal trends. Figure 4a illustrates the strong regional variability of the total solar heat input through sea ice into the ocean ($Q_T(x, y)$) ranging from 20 to 100 MJ m^{-2} for the given period. The mean total solar heat input per grid cell in the area of the mean sea ice extent was 46 MJ m^{-2} . The maximum $Q_T(x, y)$ occurs at the edge of the marginal ice zone in the Canadian Arctic Archipelago (up to 110 MJ m^{-2}) and the East Siberian Sea and Chukchi Sea (up to 80 MJ m^{-2}). In contrast, excluding ice edge effects, the minimum $Q_T(x, y)$ was found in the Central Arctic, a MYI dominated region of low transmittance.

The mean trend of $Q_T(x, y)$ was $1.5\% \text{ a}^{-1}$ (excluding sea ice edge effects) with a maximum of $+4\% \text{ a}^{-1}$ in the East Siberian Sea and southern part of the North American and Russian Arctic Basin (Figs. 4b and 5a). The reason is likely the prolongation

Seasonal cycle of solar energy fluxes through Arctic sea ice

S. Arndt and M. Nicolaus

Title Page

Abstract

Introduction

Conclusions

References

Tables

Figures



Back

Close

Full Screen / Esc

Printer-friendly Version

Interactive Discussion



Seasonal cycle of solar energy fluxes through Arctic sea ice

S. Arndt and M. Nicolaus

Title Page

Abstract

Introduction

Conclusions

References

Tables

Figures



Back

Close

Full Screen / Esc

Printer-friendly Version

Interactive Discussion



Comparing our results to the development of the solar heat input into the ice presented by Perovich et al. (2011, Fig. 2), a weaker trend in the contribution of solar heat input to the ocean (up to $1.5\% \text{ a}^{-1}$) compared to the one of solar heat input through sea ice (up to $4\% \text{ a}^{-1}$) is evident. This difference might be an indication of an increasing bottom and internal melt during the last decades and thus, affecting the sea ice mass balance. An increasing light absorption of Arctic sea ice due to more seasonal and less multi year ice was also found by Nicolaus et al. (2012).

The trend towards more light transmission through sea ice, does not only impact the light conditions right at the bottom of the sea ice, but also affects the horizontal and vertical light field in the ice covered ocean. More light at the bottom of sea ice will deepen the euphotic zone, as more light penetrates deeper into the ocean (Frey et al., 2011; Katlein et al., 2014). It contributes to an increase in mixed layer temperature, and provides more energy for primary production and biogeochemical processes in and beneath the sea ice. However, it has to be noted that an increase in light availability does not necessarily increase biological activity, but might also be harmful (Leu et al., 2010). Consequently, sea ice bottom and internal melt are likely to become more important for sea ice mass balance (Nicolaus et al., 2012), which again might result in an additional increase in transmittance. That feedback process can be trigger a transmittance-melt feedback.

Our calculated trends are based on constant pond fractions before 2000. Speculation of even less ponds, might even increase the trends. The increasing melt pond fraction on Arctic sea ice between 2000 and 2011 has been also shown in Rösel and Kaleschke (2012).

All findings are based on results that were corrected for the trend in sea ice concentration. However, to point towards the future importance of such heat fluxes, it is important to consider that those sea ice concentration trends differ significantly for different months. While the trend is $-0.1\% \text{ a}^{-1}$ for September, it is only $-0.06\% \text{ a}^{-1}$ for June, the months when the largest impact on absolute fluxes is observed. In April and May, when the most significant relative changes are observed, and when the impact

for biological primary production is expected to be largest, the trend in sea ice concentration is even positive with $+0.04\% \text{ a}^{-1}$. Hence, the importance for energy fluxes through sea ice, and their future developments, remains highly relevant also for the coming years and in a more and more seasonal Arctic sea ice cover.

4.2 Comparisons with in-situ measurements

A validation for the calculated trends and spatial variability is almost impossible as insufficient field data with adequate spatial and temporal coverage are available. However, some comparisons with time series of light transmission from different field studies may be performed to identify major uncertainties.

Here we compare, surface and transmitted solar irradiance of the presented method with in-situ measurements during the Transpolar Drift of Tara from 29 April to 28 August 2007 (Nicolaus et al., 2010a). Nearest-neighbor grid points within 0.5° of the daily Tara position were extracted from the presented data set and averaged. Figure 6a (red and green lines) shows a comparison of the time series of transmitted solar irradiance from both data sets. Until 8 June, the transmitted solar irradiance under sea ice varies only little around 0.5 W m^{-2} for both, the calculated and the measured time series. Afterwards until end of June, the measured transmitted fluxes increased steadily towards 10 W m^{-2} , whereas calculated fluxes were highly variable with most values below 4 W m^{-2} . Hence, the total solar heat input through the sea ice to the ocean from 1 May to 16 July 2007 was 21.4 MJ m^{-2} for the observed Tara data, whereas the calculated data resulted in a 17% lower total heat flux of 17.7 MJ m^{-2} . During summer (16 July to 14 August), under-ice fluxes cannot be compared reasonably since the sensor at Tara was strongly influenced by biological processes, causing an increased absorption and reduced transmitted fluxes. After 14 August, the measured transmitted heat flux increased rapidly to about 6 W m^{-2} , comparable to the calculated one. Finally, the decrease in solar elevation caused decreasing transmitted fluxes in both data sets, resulting in similar heat fluxes of $0.28 \times 10^3 \text{ MJ m}^{-2}$ after 14 August.

Seasonal cycle of solar energy fluxes through Arctic sea ice

S. Arndt and M. Nicolaus

Title Page

Abstract

Introduction

Conclusions

References

Tables

Figures

◀

▶

◀

▶

Back

Close

Full Screen / Esc

Printer-friendly Version

Interactive Discussion



Seasonal cycle of solar energy fluxes through Arctic sea ice

S. Arndt and M. Nicolaus

Title Page

Abstract

Introduction

Conclusions

References

Tables

Figures

◀

▶

◀

▶

Back

Close

Full Screen / Esc

Printer-friendly Version

Interactive Discussion



Main reason for these differences is the timing of the phases describing the surface characteristics. While both data sets have a coincident EMO on 9 June, large differences are evident for the later phase transitions: the observed MO at Tara was on 21 June whereas the calculated MO for the center position was 17 days later on 8 July.

Taking also the other 8 neighbors in account, mean MO was on 13 June. This shows that there is a difference of 25 days in MO on the 10 km grid. As presented above, the transmitted heat flux strongly depends on the timing of the different melt phases by Markus et al. (2009). EFO was observed on 15 August during Tara, whereas the satellite data maintains summer melt conditions until 14 September. However, the total solar heat input through sea ice was similar for both data sets. Conclusively, the solar radiation flux under Arctic sea ice strongly depends on the timing of EMO and MO, while the timing of EFO and FO seems to be of less importance. The timing of melt onset has also a large influence on the total amount of light absorption, as shown in Stroeve et al. (2014). Consider the ongoing lengthening of the melt season by up to two weeks per decade (by a later EMO), their calculations suggest an albedo increase of 9 % per decade.

In a second validation step, the heat fluxes were re-calculated using the onset dates as observed during Tara instead of those by Markus et al. (2009) (Fig. 6, black lines). This eliminated the impact of the onset dates on the results. Nevertheless, the calculated total solar heat input through sea ice was still differing by 18 % (25.4 MJ m^{-2}) from the Tara fluxes until 16 July (Fig. 6a) due to an unexpected peak in $Q_T(x, y)$ in July. In addition, the calculated time series showed still a large day-to-day variability, including much higher transmittances than observed at Tara. The main reason for this is the alternation of sea ice types (FYI and MYI), whereas the Tara floe consisted of MYI only. Consequently, the strong differences in optical properties of FYI and MYI, as parameterized here, strongly contribute to the overall energy budget. To overcome this problem, FYI/MYI fractions per grid cell (Kwok, 2004) could be used instead of the presented discrete distinction. However, such a data set is not yet available for the given time span.

Seasonal cycle of solar energy fluxes through Arctic sea ice

S. Arndt and M. Nicolaus

Title Page

Abstract

Introduction

Conclusions

References

Tables

Figures

◀

▶

◀

▶

Back

Close

Full Screen / Esc

Printer-friendly Version

Interactive Discussion

the entire year 2011. The strongest increase of 33 % compared to the reference melt onset dates was found for May, while the strongest absolute increase of 3.1×10^{19} J was found in June. Shifting the melt season another 7 days backwards, Q_T increases in total by 24 % to about 66.3×10^{19} J for the year. This increase is more than double compared to the 7-day-shift (Table 3). The pronounced increase is most evident in May, when 90 % more light transmission was found than in the reference system. The strongest absolute increase of 6.2×10^{19} J (transmittance from 0.054 to 0.067) was derived for June. The spatial distribution of the impact of the 14 days earlier EMO and MO showed the largest increase of solar heat input to the upper ocean in the marginal ice zone, adding up to more than 100 % (Fig. 7a).

Experiment 3, extending the melt season by 14 days later EFO and FO, results in a 1 % increase of Q_T from 53.3×10^{19} J to 53.9×10^{19} J (Fig. 7b). Since the surface solar radiation is much less than between April and June, the change in the end of the melt season affects only parts of August and September (increase of 9 % from 7.02×10^{19} J to 7.65×10^{19} J).

In a fourth sensitivity study, the influence of the ice type was quantified. The reference ice cover of 2011 consists e.g. of 56 % FYI and 44 % MYI in August. Assuming that all sea ice in 2011 was MYI, the mean transmitted flux decreased by 34 % to 35.5×10^{19} J. In contrast, assuming that only FYI was present increased that value by 18 % to 62.7×10^{19} J. Hence, the transition from a MYI to FYI dominated Arctic sea ice regime results in a further increase of solar heat flux under Arctic sea ice.

Beyond those experiments, also other parameters influence the amount and seasonality of solar heat input through the ice to the ocean, in particular surface solar radiation and the melt pond fraction. Increasing the latter by 10 %, the annual heat flux increases by 5 % for the solar heat input to the upper ocean. The effect approximately scales linearly, and increasing the melt pond fraction by 20 % results in an increase of the heat flux by 10 %. Changes in the solar surface radiation as well as in sea ice concentration have also a linear influence on the solar radiation flux under Arctic sea

Seasonal cycle of solar energy fluxes through Arctic sea ice

S. Arndt and M. Nicolaus

Title Page

Abstract

Introduction

Conclusions

References

Tables

Figures

◀

▶

◀

▶

Back

Close

Full Screen / Esc

Printer-friendly Version

Interactive Discussion



More investigations of bio-geo-physical connections will be needed to better quantify the effects of the changing physical environment on the ecosystem and element cycles, and vice versa. Additional work will also be needed to improve Arctic-wide snow depth and sea ice thickness data products. Those products should on a good description of surface properties during the spring-summer-transition, when the largest uncertainties were found. Such time series might become available from new data products merging observations from different satellites and sensor types (e.g. SMOS, CryoSat-2, AMSR-E), and potentially also numerical models. The non-existence of such reliable long-term and Arctic-wide data sets was the main reason to develop the presented method, based on available parameters. Otherwise, the application of a radiation transfer model with adequate input (forcing) data would have been an obvious alternative.

Acknowledgements. We are most grateful to Jim Maslanik (University of Colorado Boulder), Thorsten Markus and Jeffrey Miller (both NASA Goddard Space Flight Center), Thomas Lavergne (OSISAF, Met Norway), and Anja Rösel and Lars Kaleschke (both University of Hamburg) for data provision and support through manifold discussions on their data products and processing details. We thank Christian Katlein (Alfred-Wegener-Institut Helmholtz-Zentrum für Polar- und Meeresforschung) and Martin Claussen (Max Planck Institute for Meteorology) for constructive comments on the manuscript. The study was funded through the Remote Sensing Alliance of the Helmholtz Association and the Alfred-Wegener-Institut Helmholtz-Zentrum für Polar- und Meeresforschung.

References

- Andersen, S., Breivik, L. A., Eastwood, S., Godøy, Ø., Lind, M., Porcires, M., and Schyberg, H.: OSI SAF Sea Ice Product Manual, v3. 5, EUMETSAT OSI SAF, Ocean and Sea Ice Satellite Application Facility, Tech. Rep. SAF/OSI/met. no/TEC/MA/125, Copenhagen, 2007.
- Arrigo, K. R., Perovich, D. K., Pickart, R. S., Brown, Z. W., van Dijken, G. L., Lowry, K. E., Mills, M. M., Palmer, M. A., Balch, W. M., Bahr, F., Bates, N. R., Benitez-Nelson, C., Bowler, B., Brownlee, E., Ehn, J. K., Frey, K. E., Garley, R., Laney, S. R., Lubelczyk, L., Mathis, J., Matsuoka, A., Mitchell, B. G., Moore, G. W. K., Ortega-Retuerta, E., Pal, S.,

Seasonal cycle of solar energy fluxes through Arctic sea ice

S. Arndt and M. Nicolaus

Title Page

Abstract

Introduction

Conclusions

References

Tables

Figures

◀

▶

◀

▶

Back

Close

Full Screen / Esc

Printer-friendly Version

Interactive Discussion



Polashenski, C. M., Reynolds, R. A., Schieber, B., Sosik, H. M., Stephens, M., and Swift, J. H.: Massive phytoplankton blooms under Arctic sea ice, *Science*, 336, 1408–1408, doi:10.1126/Science.1215065, 2012.

Comiso, J. C.: Large decadal decline of the Arctic multiyear ice cover, *J. Climate*, 25, 1176–1193, 2012.

Deal, C., Jin, M. B., Elliott, S., Hunke, E., Maltrud, M., and Jeffery, N.: Large-scale modeling of primary production and ice algal biomass within arctic sea ice in 1992, *J. Geophys. Res.-Oceans*, 116, C07004, doi:10.1029/2010jc006409, 2011.

Dee, D. P., Uppala, S. M., Simmons, A. J., Berrisford, P., Poli, P., Kobayashi, S., Andrae, U., Balmaseda, M. A., Balsamo, G., and Bauer, P.: The ERA – interim reanalysis: configuration and performance of the data assimilation system, *Q. J. Roy. Meteor. Soc.*, 137, 553–597, 2011.

Frey, K. E., Perovich, D. K., and Light, B.: The spatial distribution of solar radiation under a melting Arctic sea ice cover, *Geophys. Res. Lett.*, 38, L22501, doi:10.1029/2011GL049421, 2011.

Haas, C., Pfaffling, A., Hendricks, S., Rabenstein, L., Etienne, J. L., and Rigor, I.: Reduced ice thickness in Arctic Transpolar Drift favors rapid ice retreat, *Geophys. Res. Lett.*, 35, L17501, doi:10.1029/2008gl034457, 2008.

Hudson, S. R., Granskog, M. A., Sundfjord, A., Randelhoff, A., Renner, A. H. H., and Divine, D. V.: Energy budget of first-year Arctic sea ice in advanced stages of melt, *Geophys. Res. Lett.*, 40, 2679–2683, doi:10.1002/grl.50517, 2013.

Katlein, C., Nicolaus, M., and Petrich, C.: The anisotropic scattering coefficient of sea ice, *J. Geophys. Res. Oceans*, 119, 842–855, doi:10.1002/2013JC009502, 2014.

Krishfield, R., Toole, J., Proshutinsky, A., and Timmermans, M. L.: Automated ice-tethered profilers for seawater observations under pack ice in all seasons, *J. Atmos. Ocean. Tech.*, 25, 2091–2105, doi:10.1175/2008jtecho587.1, 2008.

Kwok, R.: Annual cycles of multiyear sea ice coverage of the Arctic Ocean: 1999–2003, *J. Geophys. Res.*, 109, C11004, doi:10.1029/2003JC002238, 2004.

Lavergne, T., Killie, M. A., Eastwood, S., and Breivik, L.-A.: Extending the CryoClim Arctic Sea Ice Extent Time Series with Operational OSI SAF Products from 2008 Onwards, Norwegian Meteorological Institute Note, 7, Oslo, 2010.

Seasonal cycle of solar energy fluxes through Arctic sea ice

S. Arndt and M. Nicolaus

Title Page

Abstract

Introduction

Conclusions

References

Tables

Figures

◀

▶

◀

▶

Back

Close

Full Screen / Esc

Printer-friendly Version

Interactive Discussion



Leu, E., Wiktor, J., Soreide, J. E., Berge, J., and Falk-Petersen, S.: Increased irradiance reduces food quality of sea ice algae, *Mar. Ecol. Prog. Ser.*, 411, 49–60, doi:10.3354/meps08647 2010.

Markus, T., Stroeve, J. C., and Miller, J. A.: Recent changes in Arctic sea ice melt onset, freezeup, and melt season length, *J. Geophys. Res.*, 114, C12024, doi:10.1029/2009JC005436, 2009.

Maslanik, J. A., Fowler, C., Stroeve, J., Drobot, S., Zwally, J., Yi, D., and Emery, W.: A younger, thinner Arctic ice cover: increased potential for rapid, extensive sea-ice loss, *Geophys. Res. Lett.*, 34, L24501, doi:10.1029/2007gl032043, 2007.

Maslanik, J. A., Stroeve, J., Fowler, C., and Emery, W.: Distribution and trends in Arctic sea ice age through spring 2011, *Geophys. Res. Lett.*, 38, L13502, doi:10.1029/2011gl047735, 2011.

Mundy, C. J., Barber, D. G., and Michel, C.: Variability of snow and ice thermal, physical and optical properties pertinent to sea ice algae biomass during spring, *J. Marine Syst.*, 58, 107–120, doi:10.1016/J.Jmarsys.2005.07.003, 2005.

Mundy, C. J., Ehn, J. K., Barber, D. G., and Michel, C.: Influence of snow cover and algae on the spectral dependence of transmitted irradiance through Arctic landfast first-year sea ice, *J. Geophys. Res.-Oceans*, 112, C03007, doi:10.1029/2006jc003683, 2007.

Nicolaus, M. and Katlein, C.: Mapping radiation transfer through sea ice using a remotely operated vehicle (ROV), *The Cryosphere*, 7, 763–777, doi:10.5194/tc-7-763-2013, 2013.

Nicolaus, M., Haas, C., Bareiss, J., and Willmes, S.: A model study of differences of snow thinning on Arctic and Antarctic first-year sea ice during spring and summer, *Ann. Glaciol.*, 44, 147–153, 2006.

Nicolaus, M., Gerland, S., Hudson, S. R., Hanson, S., Haapala, J., and Perovich, D. K.: Seasonality of spectral albedo and transmittance as observed in the Arctic Transpolar Drift in 2007, *J. Geophys. Res.-Oceans*, 115, C11011, doi:10.1029/2009jc006074, 2010a.

Nicolaus, M., Hudson, S. R., Gerland, S., and Munderloh, K.: A modern concept for autonomous and continuous measurements of spectral albedo and transmittance of sea ice, *Cold Reg. Sci. Technol.*, 62, 14–28, 2010b.

Nicolaus, M., Katlein, C., Maslanik, J., and Hendricks, S.: Changes in Arctic sea ice result in increasing light transmittance and absorption, *Geophys. Res. Lett.*, 39, L24501, doi:10.1029/2012GL053738, 2012.

Seasonal cycle of solar energy fluxes through Arctic sea ice

S. Arndt and M. Nicolaus

Title Page

Abstract

Introduction

Conclusions

References

Tables

Figures



Back

Close

Full Screen / Esc

Printer-friendly Version

Interactive Discussion



Nicolaus, M., Arndt, S., Katlein, C., Maslanik, J., and Hendricks, S.: Correction to “Changes in Arctic sea ice result in increasing light transmittance and absorption”, *Geophys. Res. Lett.*, 40, 2699–2700, doi:10.1002/grl.50523, 2013.

Perovich, D. K.: The Optical Properties of Sea Ice, DTIC Document, 96-1, 25 pp., Hanover, N. H., May 1996.

Perovich, D. K.: On the aggregate-scale partitioning of solar radiation in Arctic sea ice during the Surface Heat Budget of the Arctic Ocean (SHEBA) field experiment, *J. Geophys. Res.-Oceans*, 110, C03002, doi:10.1029/2004jc002512, 2005.

Perovich, D. K. and Polashenski, C.: Albedo evolution of seasonal Arctic sea ice, *Geophys. Res. Lett.*, 39, L08501, doi:10.1029/2012GL051432, 2012.

Perovich, D. K. and Richter-Menge, J. A.: Loss of Sea Ice in the Arctic*, *Annual Review of Marine Science*, 1, 417–441, 2009.

Perovich, D. K., Roesler, C. S., and Pegau, W. S.: Variability in Arctic sea ice optical properties, *J. Geophys. Res.-Oceans*, 103, 1193–1208, doi:10.1029/97jc01614, 1998.

Perovich, D. K., Grenfell, T. C., Light, B., and Hobbs, P. V.: Seasonal evolution of the albedo of multiyear Arctic sea ice, *J. Geophys. Res.-Oceans*, 107, 8044, doi:10.1029/2000jc000438, 2002.

Perovich, D. K., Nghiem, S. V., Markus, T., and Schweiger, A.: Seasonal evolution and inter-annual variability of the local solar energy absorbed by the Arctic sea ice–ocean system, *J. Geophys. Res.-Oceans*, 112, C03005, doi:10.1029/2006jc003558, 2007.

Perovich, D. K., Jones, K. F., Light, B., Eicken, H., Markus, T., Stroeve, J., and Lindsay, R.: Solar partitioning in a changing Arctic sea-ice cover, *Ann. Glaciol.*, 52, 192–196, 2011.

Popova, E. E., Yool, A., Coward, A. C., Dupont, F., Deal, C., Elliott, S., Hunke, E., Jin, M. B., Steele, M., and Zhang, J. L.: What controls primary production in the Arctic Ocean?, Results from an intercomparison of five general circulation models with biogeochemistry, *J. Geophys. Res.-Oceans*, 117, C00d12, doi:10.1029/2011jc007112, 2012.

Rösel, A. and Kaleschke, L.: Exceptional melt pond occurrence in the years 2007 and 2011 on the Arctic sea ice revealed from MODIS satellite data, *J. Geophys. Res.-Oceans*, 117, C05018, doi:10.1029/2011jc007869, 2012.

Rösel, A., Kaleschke, L., and Birnbaum, G.: Melt ponds on Arctic sea ice determined from MODIS satellite data using an artificial neural network, *The Cryosphere*, 6, 431–446, doi:10.5194/tc-6-431-2012, 2012.

Stroeve, J. C., Markus, T., Boisvert, L., Miller, J., and Barrett, A.: Changes in Arctic melt season and implications for sea ice loss, *Geophys. Res. Lett.*, 41, 1216–1225, doi:10.1002/2013gl058951, 2014.

5 Wang, C., Granskog, M. A., Gerland, S., Hudson, S. R., Perovich, D. K., Nicolaus, M., Ivan Karlsen, T., Fossan, K., and Bratrein, M.: Autonomous observations of solar energy partitioning in first-year sea ice in the Arctic Basin, *J. Geophys. Res.-Oceans*, 119, 2066–2080, 2014.

TCD

8, 2923–2956, 2014

Seasonal cycle of solar energy fluxes through Arctic sea ice

S. Arndt and M. Nicolaus

Title Page

Abstract

Introduction

Conclusions

References

Tables

Figures

⏪

⏩

◀

▶

Back

Close

Full Screen / Esc

Printer-friendly Version

Interactive Discussion



Seasonal cycle of solar energy fluxes through Arctic sea ice

S. Arndt and M. Nicolaus

Table 2. Transmittances of different sea ice and surface types. Abbreviations: FYI: first year ice, MYI: multi year ice, Phase I: winter, MO: melt onset, Phase IV: summer, FO: freeze onset, Threshold: transition from open ocean to sea ice and vice versa.

	Phase I (winter)	At MO	Phase IV (summer)	At FO	Threshold
FYI, pond covered sea ice	0.002	0.04	0.087	0.04	0.4
MYI, pond covered sea ice	0.002	0.02	0.05	0.02	0.4
FYI, bare ice/snow	0.001	0.017	0.04	0.017	0.17
FYI, melt ponds			0.22		
MYI, bare ice/snow	0	0.004	0.01	0.004	0.07
MYI, melt ponds			0.15		
Open ocean			0.93		

Title Page

Abstract

Introduction

Conclusions

References

Tables

Figures

◀

▶

◀

▶

Back

Close

Full Screen / Esc

Printer-friendly Version

Interactive Discussion



Seasonal cycle of solar energy fluxes through Arctic sea ice

S. Arndt and M. Nicolaus

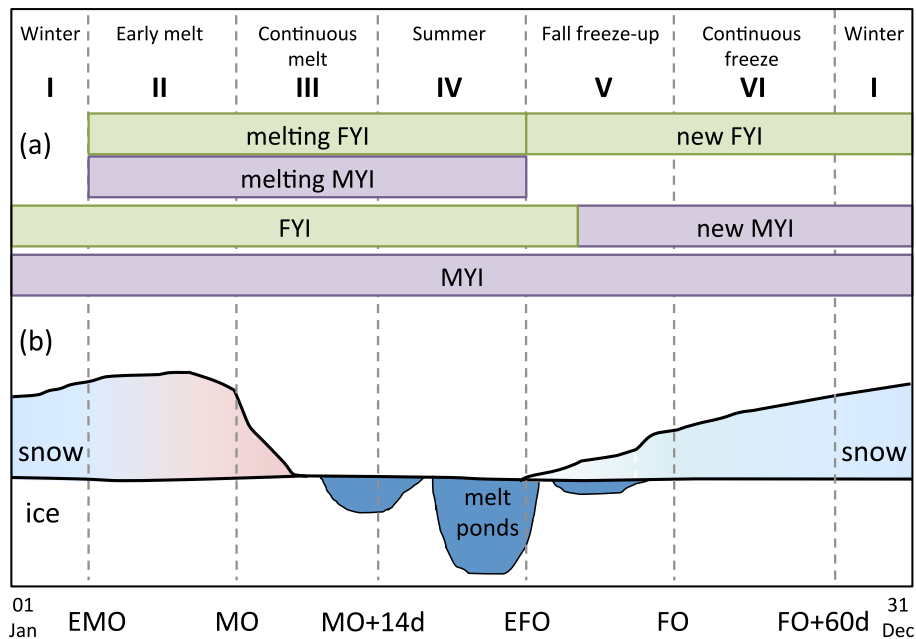


Figure 1. Classification of sea ice (a) types and (b) surface properties as used in this study. The timing of each phase results from the status of the sea ice. Depending on the season, different sea ice types co-exist. Abbreviations: FYI: first year ice, MYI: multi year ice, EMO: early melt onset, MO: melt onset, EFO: early freeze onset, FO: freeze onset.

Seasonal cycle of solar energy fluxes through Arctic sea ice

S. Arndt and M. Nicolaus

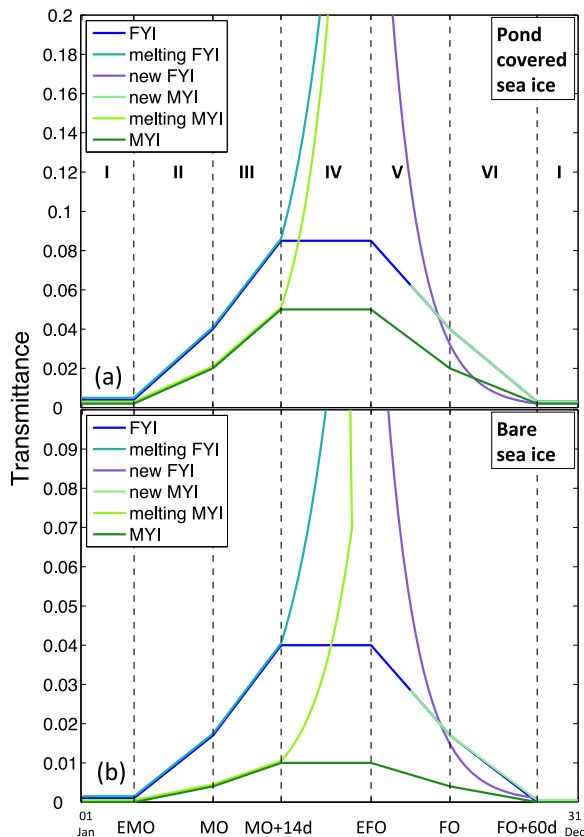


Figure 2. (a) Total transmittance of sea ice during each phase (Fig. 1). In this figure, melt pond concentrations of 26% are assumed for first year ice (FYI) and 29% are assumed for multi year ice (MYI). (b) Transmittance of bare ice during each phase (see Fig. 1). Transmittances of single ice classes are given in Table 1. Abbreviations: see Fig. 1.

[Title Page](#)
[Abstract](#)
[Introduction](#)
[Conclusions](#)
[References](#)
[Tables](#)
[Figures](#)
[◀](#)
[▶](#)
[◀](#)
[▶](#)
[Back](#)
[Close](#)
[Full Screen / Esc](#)
[Printer-friendly Version](#)
[Interactive Discussion](#)

Seasonal cycle of solar energy fluxes through Arctic sea ice

S. Arndt and M. Nicolaus

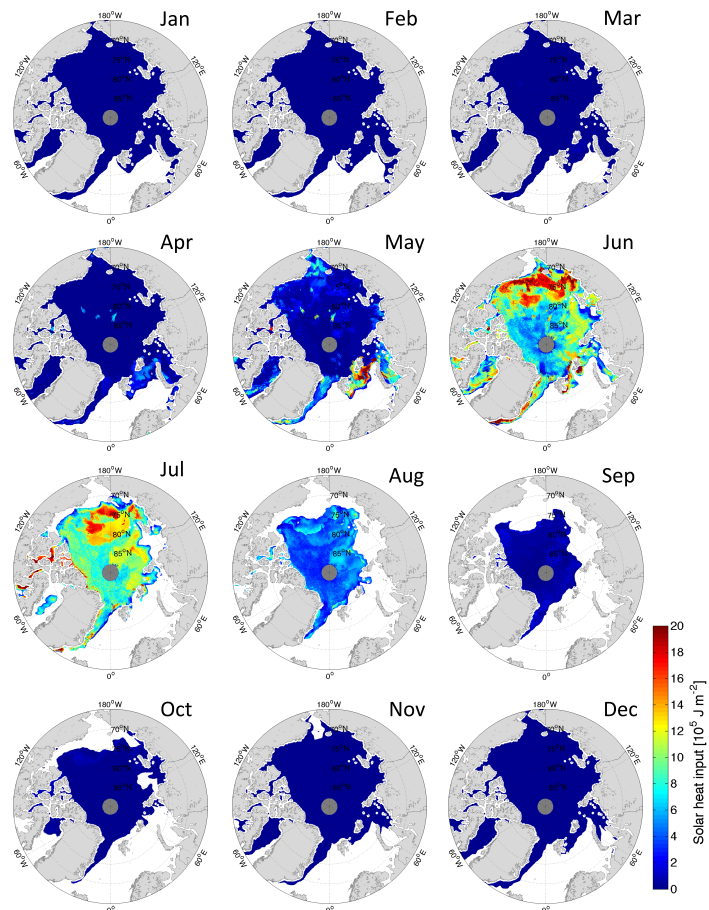


Figure 3. Monthly mean of total solar heat input ($Q_T(x,y)$) under Arctic sea ice (ice covered areas only) for the year 2011.

[Title Page](#)
[Abstract](#)
[Introduction](#)
[Conclusions](#)
[References](#)
[Tables](#)
[Figures](#)
[Back](#)
[Close](#)
[Full Screen / Esc](#)
[Printer-friendly Version](#)
[Interactive Discussion](#)


Seasonal cycle of solar energy fluxes through Arctic sea ice

S. Arndt and M. Nicolaus

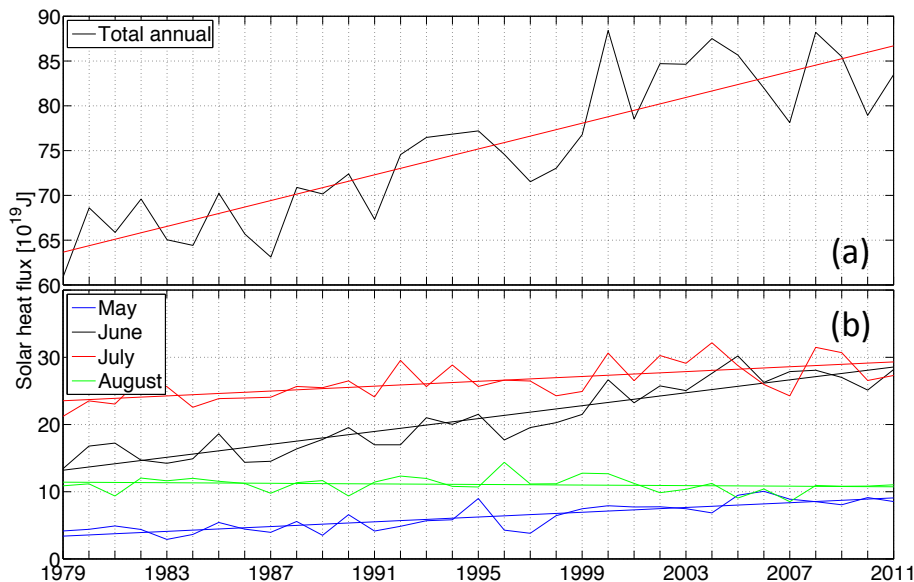


Figure 5. (a) Arctic-wide total solar heat flux under sea ice (Q_+) (black) and its trend (red) from 1979 to 2011. (b) Monthly Arctic-wide solar heat input for May to August and its trend from 1979 to 2011. The data are corrected for the trend in sea ice concentration. Areas that were not ice covered at any time in 2011 or in the certain month in 2011 are excluded from the analyses.

Title Page

Abstract

Introduction

Conclusions

References

Tables

Figures

◀

▶

◀

▶

Back

Close

Full Screen / Esc

Printer-friendly Version

Interactive Discussion



